ELSEVIER

27 March 1998

Chemical Physics Letters 285 (1998) 438–448

CHEMICAL PHYSICS LETTERS

Corrections to the semiclassical approximation by numerical evaluation of real time path integrals in complex space

Fernando S. dos Aidos

Departamento de Física, Universidade de Coimbra, 3000 Coimbra, Portugal

Received 22 August 1997; in final form 5 January 1998

Abstract

A numerical method for evaluating real time path integrals by analytical continuation of the coordinate space variables into the complex plane is presented. With this method, a Monte Carlo gaussian sampling function around the classical paths is obtained. The function to be sampled is smooth near the stationary path and good Monte Carlo convergence is expected.

1. Introduction

Path integrals have been successfully applied for the last three decades to scattering theory [1], where the semiclassical approximation leads to an appealing description of the scattering processes in terms of classical trajectories. In order to go beyond the semiclassical approach in this formalism, it is necessary to be able to perform the numerical evaluation of a real time path integral. An efficient method to carry out such a calculation should profit from the success of the semiclassical approach and build the quantum formalism upon the semiclassical results. For the method to be useful, it should also allow for the possibility of including an appreciable number of time slices in the calculation. Unfortunately, although several methods for the numerical evaluation of real time path integrals have been developed [2–16], their application to long time propagation is still problematic due to loss of efficiency of the Monte Carlo sampling of the oscillatory integrand as the dimensionality of the integral increases [17].

In this Letter, we present a method for the numerical evaluation of a real time path integral which is based on the analytical continuation of the action integral into the coordinate complex plane. The idea of going into the coordinate complex plane is not new. It is the basis of the coordinate rotation formalism [11,12] where analytical continuation is performed in such a way that the imaginary kinetic exponent becomes real and negative, thus privileging the straight line trajectories. Analytical continuation was also used by Mak and Chandler [9,10], in the context of the stationary phase Monte Carlo (SPMC) method developed by Doll et al. [5,6], in order to obtain contributions from the regions around complex points of stationary phase by crossing them along the path of steepest descent.

Our method assumes that the stationary points are real and sufficiently far apart from each other, although it can easily be extended to accommodate complex stationary points as will be shown in Section 3. The contour of

0009-2614/98/$19.00
PII S0009-2614(98)00086-4

integration is then changed so that each stationary point is crossed along the path of steepest descent used in the semiclassical approximation and we do not need the SPMC method to obtain convergence. The emerging procedure requires the sampling of the paths around the classical trajectories with a gaussian distribution function. It is not as general as the previously developed stationary-phase-based methods [4–10], as it demands the stationary paths to be known and far apart from each other, but the numerical effort that it requires is lighter and the Monte Carlo convergence expected to be better. Our assumptions may seem too restrictive for bound state problems, as there will normally be many real classical trajectories connecting two end points in a given time interval, depending on the number of times the particle bounces off the potential walls. However, for scattering problems, the classical trajectories will generally be very few [18] and often well apart from each other. Even for bound state problems it seems reasonable, on physical grounds, that only the low energy classical trajectories will contribute to low energy phenomena, and this should restrict the real classical paths to a manageable number. Complex classical trajectories generally correspond to highly damped phenomena and should only be used whenever there are no real classical trajectories available.

We note that, contrary to Mak and Chandler [9], we do not need to include a filter function in the integral as proposed by the SPMC method [5]. As long as the propagator is not too far from the semiclassical limit, the integration contour that we choose, a) provides the gaussian distribution function and b) automatically eliminates the oscillations of the sampled function in the range of the distribution function. In this way, we avoid the free parameter ϵ used in the SPMC method that controls the efficiency of the filter and the Monte Carlo convergence. In our method, Monte Carlo convergence is controlled by the size of the second derivative of the action as compared to the higher order terms. Consequently, if the semiclassical approximation is reasonable, the effect of the higher order terms must be small, and the function that is being sampled by Monte Carlo must be smooth around the stationary paths. This feature of our method will hopefully allow for accurate long time propagation calculations for "sufficiently semiclassical" problems such as the ones that often arise in studying scattering processes.

The method is described in Section 2, first in its one dimensional version, and then in the general form, for a multi-dimensional integral. We present the results from several numerical tests in Section 3 and a discussion of the method in Section 4.

2. The method

Basically, our method consists in applying the technique used in the calculation of the semiclassical path integral to the evaluation of the exact expression.

A path integral can be written as a multi-dimensional integral in configuration space [19,20]

$$K \simeq C_N \int \mathrm{d}\boldsymbol{r}_1 \cdots \int \mathrm{d}\boldsymbol{r}_N \exp\left[\frac{i}{\hbar} S(\boldsymbol{r}_1, \ldots, \boldsymbol{r}_N)\right]. \tag{1}$$

We start by applying our method to the calculation of a one dimensional integral for the sake of clarity. The multi-dimensional case will be treated subsequently. In the remainder of this Letter, the $1/\hbar$ factor in the exponent and the constant factor C_N will be suppressed.

In one dimension, our problem consists in evaluating the integral

$$K = \int_{-\infty}^{\infty} \mathrm{d}x \exp[\mathrm{i}S(x)], \tag{2}$$

where $S(x)$ is a real function of the coordinate x. We assume that the function $S(x)$ describes a system for

which the semiclassical approximation provides a reasonable result. We also assume, for the moment, that there is only one stationary point x_s such that

$$S_1(x_s) = S'(x_s) = 0 \tag{3}$$

and

$$S_2(x_s) = S''(x_s) > 0. \tag{4}$$

Expanding S around the stationary point we obtain

$$S(x) = S(x_s) + \tfrac{1}{2}S_2(x_s)(x - x_s)^2 + S_{3+}(x). \tag{5}$$

A first estimate for the value of K is provided by the semiclassical approximation, obtained by neglecting $S_{3+}(x)$,

$$K \simeq K_{sc} = \exp[iS(x_s)] \int_{-\infty}^{\infty} dx \exp\left[i\tfrac{1}{2}S_2(x_s)(x - x_s)^2\right]. \tag{6}$$

Evaluating this integral, we obtain

$$K_{sc} = \left(\frac{2\pi}{S_2(x_s)}\right)^{1/2} \exp[i(S(x_s) + \pi/4)]. \tag{7}$$

If the semiclassical approximation is reasonable, $S_2(x_s)$ must be large enough for $S_{3+}(x)$ to be small in the region which provides most of the contribution to the integral K, near x_s. Consequently, the part of the integrand that is left out in the semiclassical calculation should be close to unity around x_s, thus exhibiting no oscillations in that region.

We are now going to apply to the evaluation of the exact integral K, defined in Eq. (2), the same technique that was used to calculate the semiclassical integral in Eq. (6). Basically, this corresponds to a deformation of the integration contour in the complex plane in order to turn the purely imaginary quadratic exponent into a negative real one and thus obtain a gaussian that can be used as a probability distribution function in a Monte Carlo calculation.

We start by changing variables in Eq. (2)

$$x \to y = x - x_s, \tag{8}$$

and analytically continue y into the complex plane. Assuming that $S(x)$ is analytic in the regions A_1 and A_2 shown in Fig. 1, we use Cauchy's theorem to deform the contour of integration and obtain

$$K = \int_{-\infty}^{-R} dy \exp[iS(x_s + y)] + \int_{C_1(R)} dy \exp[iS(x_s + y)] + \int_{-R\exp(i\pi/4)}^{R\exp(i\pi/4)} dy \exp[iS(x_s + y)]$$
$$+ \int_{C_2(R)} dy \exp[iS(x_s + y)] + \int_{R}^{\infty} dy \exp[iS(x_s + y)]. \tag{9}$$

Assuming that the contributions from $C_1(R)$ and $C_2(R)$ vanish for large values of R, the integral becomes

$$K = \int_{-R_0\exp(i\pi/4)}^{R_0\exp(i\pi/4)} dy \exp[iS(x_s + y)], \tag{10}$$

where R_0 is some suitable large value of R. We now use expression (5) for S and change variables

$$y \to z = y\exp(-i\pi/4), \tag{11}$$

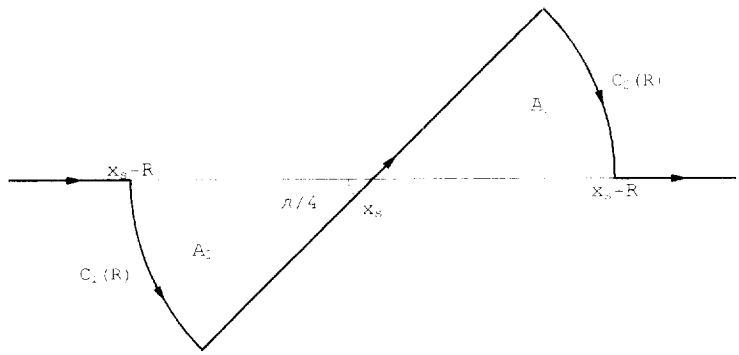

Fig. 1. Deformation of the contour of integration when $S_2(x_s) > 0$.

to obtain

$$K = \exp\left[i(S(x_s) + \pi/4)\right] \int_{-R_0}^{R_0} dz \exp\left(-\tfrac{1}{2} S_2(x_s) z^2\right) \exp\left[iS_{3+}(x_s + z\exp(i\pi/4))\right]$$

$$= K_{sc} \int_{-R_0}^{R_0} dz\, p(z) \exp\left[iS_{3+}(x_s + z\exp(i\pi/4))\right] \tag{12}$$

where $p(z)$ is given by

$$p(z) = \left(\frac{S_2(x_s)}{2\pi}\right)^{1/2} \exp\left[-\tfrac{1}{2} S_2(x_s) z^2\right]. \tag{13}$$

The integral in Eq. (12) can now be evaluated by the Monte Carlo method

$$K \simeq K_{sc} \frac{1}{N_{MC}} \sum_{k=1}^{N_{MC}} \exp\left[iS_{3+}(x_s + z_k \exp(i\pi/4))\right], \tag{14}$$

where the values of z_k are distributed according to the normalized gaussian probability function $p(z)$.

The function that is being sampled is no longer just a phase, due to the extra $\pi/4$ phase that is being added to z. It is the exponential of a function of third order in z but, for symmetry reasons, the first term to contribute to the integral is of fourth order. Therefore, this function must be close to unity near the stationary point and, as long as $S_2(x_s)$ is large enough (as we assume it should be for the semiclassical approximation to be reasonable) the Monte Carlo convergence should be good.

At this point, we note that the rotation of the integration path by the angle $\pi/4$ has turned the imaginary quadratic exponent into a negative real term. Had we chosen another rotation angle, the quadratic terms in the exponent would contain an imaginary part which would cause the Monte Carlo calculation to loose efficiency for two reasons: the gaussian would be wider and the smoothness of the function that is being sampled around the stationary point would be somewhat decreased. In some cases, it may be necessary to use a different rotation angle in order to obtain a negligible contribution from the contours $C_1(R)$ and $C_2(R)$. This does not cause the method to break down as the second example in Section 3 illustrates. However, whenever the angle $\pi/4$ can be used, it provides a better convergence.

In this derivation, we have assumed that $S_2(x_s)$ is positive. For a negative value of $S_2(x_s)$, we can proceed in

a similar way, by deforming the contour as shown in Fig. 2. The change of variables $y \to z$ is now made with a positive instead of a negative phase and the final result is

$$K = \exp[\mathrm{i}(S(x_s) - \pi/4)] \int_{-R_0}^{R_0} \mathrm{d}z \exp(-\tfrac{1}{2}|S_2(x_s)|z^2) \exp[\mathrm{i}S_{3+}(x_s + z\exp(-\mathrm{i}\pi/4))]$$

$$\simeq K_{\mathrm{sc}} \frac{1}{N_{\mathrm{MC}}} \sum_{k=1}^{N_{\mathrm{MC}}} \exp[\mathrm{i}S_{3+}(x_s + z_k \exp(-\mathrm{i}\pi/4))], \tag{15}$$

where now the semiclassical result is

$$K_{\mathrm{sc}} = \left(\frac{2\pi}{|S_2(x_s)|}\right)^{1/2} \exp[\mathrm{i}(S(x_s) - \pi/4)] \tag{16}$$

and the probability distribution for the Monte Carlo points is given by

$$p(z) = \left(\frac{|S_2(x_s)|}{2\pi}\right)^{1/2} \exp[-\tfrac{1}{2}|S_2(x_s)|z^2]. \tag{17}$$

If the function S has several stationary points then, as long as they are well apart from each other, we can proceed as above and deform the contour according to either Fig. 1 or Fig. 2 around each stationary point, depending on the sign of S_2. All that is required is that the contributions from the contours $C_1(R_0)$ and $C_2(R_0)$ be negligible for each stationary point. The final result will be the sum of the contributions from all stationary points.

For the multi-dimensional case (N_d dimensions) with one stationary path $\boldsymbol{x}_s$ for S we obtain, using an obvious matrix notation,

$$K = \int_{-\infty}^{\infty} \cdots \int_{-\infty}^{\infty} \mathrm{d}\boldsymbol{x} \exp[\mathrm{i}S(\boldsymbol{x})]$$

$$= \exp[\mathrm{i}S(\boldsymbol{x}_s)] \int_{-\infty}^{\infty} \cdots \int_{-\infty}^{\infty} \mathrm{d}\boldsymbol{x} \exp\left[\mathrm{i}\left(\tfrac{1}{2}(\boldsymbol{x} - \boldsymbol{x}_s)^T \cdot \mathbf{S}_2(\boldsymbol{x}_s) \cdot (\boldsymbol{x} - \boldsymbol{x}_s) + S_{3+}(\boldsymbol{x})\right)\right]$$

$$= \exp[\mathrm{i}S(\boldsymbol{x}_s)] \int_{-\infty}^{\infty} \cdots \int_{-\infty}^{\infty} \mathrm{d}\boldsymbol{y} \exp\left[\mathrm{i}\left(\tfrac{1}{2}\boldsymbol{y}^T \cdot \mathbf{S}_2(\boldsymbol{x}_s) \cdot \boldsymbol{y} + S_{3+}(\boldsymbol{x}_s + \boldsymbol{y})\right)\right]. \tag{18}$$

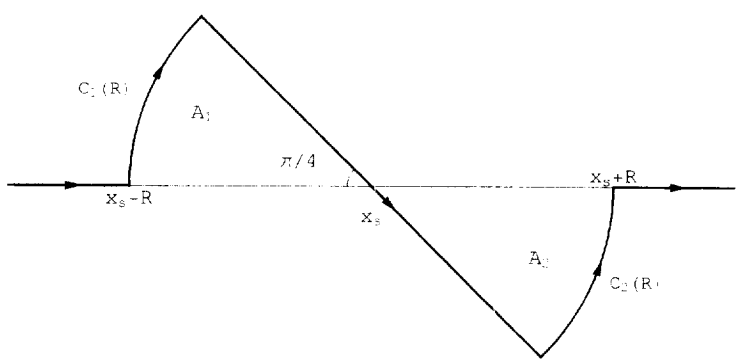

Fig. 2. Deformation of the contour of integration when $S_2(x_s) < 0$.

$\mathbf{S}_2$ is a real symmetric square matrix whose elements are the second derivatives of $S(\boldsymbol{x})$ with respect to the variables of integration x_i at the stationary path $\boldsymbol{x}_s$. It can be diagonalized by an orthogonal transformation $\mathbf{O}$

$$\boldsymbol{\Lambda} = \mathbf{O}^T \cdot \mathbf{S}_2 \cdot \mathbf{O}, \tag{19}$$

where $\boldsymbol{\Lambda}$ is the diagonal matrix with the eigenvalues of $\mathbf{S}_2$. Then

$$\boldsymbol{y}^T \cdot \mathbf{S}_2 \cdot \boldsymbol{y} = \boldsymbol{y}^T \cdot \mathbf{O} \cdot \mathbf{O}^T \cdot \mathbf{S}_2 \cdot \mathbf{O} \cdot \mathbf{O}^T \cdot \boldsymbol{y} = \left(\mathbf{O}^T \cdot \boldsymbol{y}\right)^T \cdot \boldsymbol{\Lambda} \cdot \left(\mathbf{O}^T \cdot \boldsymbol{y}\right). \tag{20}$$

The change of variables with unit Jacobian

$$\boldsymbol{y} \to \boldsymbol{y}' = \mathbf{O}^T \cdot \boldsymbol{y} \tag{21}$$

in the integral in Eq. (18) decouples the gaussians. The contour of integration can now be deformed for each variable y_i', according to either Fig. 1 or Fig. 2, depending on the sign s_i of the corresponding eigenvalue λ_i. Changing variables once more,

$$y_i' \to z_i = y_i' \exp(-\mathrm{i} s_i \pi/4) \quad \Rightarrow \quad y_i = \sum_{j=1}^{N_d} O_{ij} z_j \exp(\mathrm{i} s_j \pi/4),$$

we finally obtain for the multi-dimensional case

$$\begin{aligned} K &= K_{\mathrm{sc}} \int_{-R_{01}}^{R_{01}} \mathrm{d}z_1\, p_1(z_1) \cdots \int_{-R_{0N_d}}^{R_{0N_d}} \mathrm{d}z_{N_d}\, p_{N_d}(z_{N_d}) \exp\left[\mathrm{i} S_{3+}\left(x_{si} + \sum_{j=1}^{N_d} O_{ij} z_j \exp(\mathrm{i} s_j \pi/4)\right)\right] \\ &\simeq K_{\mathrm{sc}} \frac{1}{N_{\mathrm{MC}}} \sum_{k=1}^{N_{\mathrm{MC}}} \exp\left[\mathrm{i} S_{3+}\left(x_{si} + \sum_{j=1}^{N_d} O_{ij} z_{jk} \exp(\mathrm{i} s_j \pi/4)\right)\right], \end{aligned} \tag{22}$$

where K_{sc} is the semiclassical result

$$K_{\mathrm{sc}} = \left|\det\left(\frac{\mathbf{S}_2}{2\pi}\right)\right|^{-1/2} \exp\left[\mathrm{i}\left(S(\boldsymbol{x}_s) + \sum_{i=1}^{N_d} s_i \pi/4\right)\right] \tag{23}$$

and z_{ik} are values of the ith variable distributed according to the normalized gaussian probability function

$$p_i(z_i) = \left(\frac{|\lambda_i|}{2\pi}\right)^{1/2} \exp\left[-\tfrac{1}{2}|\lambda_i| z_i^2\right]. \tag{24}$$

If there are several well separated paths, then, as in the one dimensional case, provided that the contributions from the contours $C_{1i}(R_{0i})$ and $C_{2i}(R_{0i})$ are vanishingly small, the final result will be the sum of contributions like Eq. (22) from all stationary paths.

3. Numerical results

We have tested our method, by calculating the following three one-dimensional integrals for several values of the parameter α

$$I_1(\alpha) = \int_{-\infty}^{\infty} \mathrm{d}x \exp\left[\mathrm{i}\left(\alpha \frac{x^2}{2} + \frac{x^4}{4}\right)\right], \tag{25}$$

$$I_2(\alpha) = \int_{-\infty}^{\infty} \mathrm{d}x \exp\left[\mathrm{i}\left(\alpha \frac{x^2}{2} + \frac{x^{10}}{10}\right)\right], \tag{26}$$

$$I_3(\alpha) = \mathrm{Ai}(-\alpha) = \frac{1}{2\pi} \int_{-\infty}^{\infty} \mathrm{d}x \exp\left[\mathrm{i}\left(\alpha x - \frac{x^3}{3}\right)\right]. \tag{27}$$

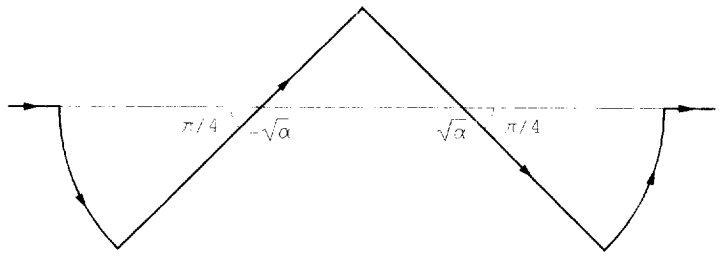

Fig. 3. Integration contour for the evaluation of $I_3(\alpha)$ for positive values of α.

For all these integrals, the semiclassical approximation should lead to good results for large values of the parameter α, while for small values of α it is expected to break down. All calculations were made with 5000 Monte Carlo points, using the Box-Muller method for sampling the gaussians. In all cases we have symmetrized the sampled function in order to improve convergence:

$$\exp\left[iS_{3-}(x_s + z\exp(i\pi/4))\right] \rightarrow \frac{\exp\left[iS_{3+}(x_s + z\exp(i\pi/4))\right] + \exp\left[iS_{3+}(x_s - z\exp(i\pi/4))\right]}{2}. \tag{28}$$

Only the real stationary point $x_s = 0$ was used in the evaluation of $I_1(\alpha)$ and $I_2(\alpha)$. All complex stationary points were discarded.

When calculating $I_2(\alpha)$, the rotation angle mentioned in Section 2 and represented in Fig. 1 cannot be larger than $\pi/10$, otherwise the contributions from the contours $C_1(R)$ and $C_2(R)$ will not vanish. We have used the maximum value $\pi/10$. Unlike $\pi/4$, this rotation angle does not totally convert the pure imaginary quadratic exponent into a negative real term. There is still an imaginary quadratic component left. This imaginary term will be added to S_{3+} in the exponent of the sampled function, while the negative real quadratic term alone will make up the gaussian distribution function.

The Airy function, integral $I_3(\alpha)$, was calculated for positive and for negative values of α.

For positive values, there are two real stationary points

$$x_{s+} = \sqrt{\alpha} \quad \text{and} \quad x_{s-} = -\sqrt{\alpha} \tag{29}$$

and the integrals along the contours C_{2-} and C_{1-} do not vanish. Therefore, we have used the contour represented in Fig. 3 taking proper care to truncate the integral around x_{s-} for $z > \sqrt{2}\,\alpha$ and the integral around x_{s+} for $z < -\sqrt{2}\,\alpha$. The symmetry properties of the integrand have been used to write the final result as a Monte Carlo calculation around only one stationary point. In the semiclassical calculation we have also used the integration contour in Fig. 3, which imposes the above mentioned truncations. The results obtained in this way are better than the values provided by the standard semiclassical expression for small values of α. For large values of α, the results are the same.

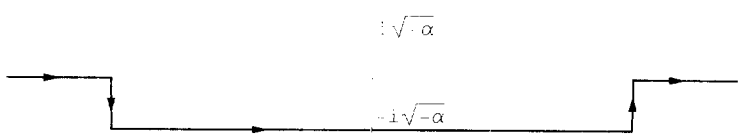

Fig. 4. Integration contour for the evaluation of $I_3(\alpha)$ for negative values of α.

Table 1
Results of the evaluation of the integral defined in Eq. (25). For each value of the constant α, the real values are shown on the first line and the imaginary values on the second. Column S shows the semiclassical results (Eq. (7)), column MC the values obtained by the method described in this Letter (Eq. (14)), column E the exact values, column ΔS the semiclassical deviation $|E-S|$ and column ΔMC the statistical deviation in the Monte Carlo calculation

α	S	MC	E	ΔS	ΔMC
10	0.5605	0.5643	0.5645	0.0040	0.0002
	0.5605	0.5564	0.5561	0.0044	0.0002
5	0.7927	0.8113	0.8117	0.0190	0.0006
	0.7927	0.7679	0.7663	0.0264	0.001
1	1.7725	1.7149	1.7089	0.0636	0.01
	1.7725	1.1049	1.1021	0.6704	0.02
0.5	2.5066	2.0343	2.0024	0.5042	0.03
	2.5066	1.0995	1.0845	1.4221	0.03
0.1	5.6050	2.2475	2.2898	3.3152	0.08
	5.6050	1.0174	1.0114	4.5936	0.07

For negative values of α, the two stationary points are complex

$$x_{s+} = \mathrm{i}\sqrt{|\alpha|} \quad \text{and} \quad x_{s-} = -\mathrm{i}\sqrt{|\alpha|}\,. \tag{30}$$

A semiclassical evaluation is still possible if the contour is deformed according to Fig. 4. It is clear that the upper stationary point does not contribute to the integral and that the contribution from the lower stationary point can be evaluated in a similar way to the one described in Section 2. In this case, however, the contour used in the semiclassical approximation corresponds to a translation instead of a rotation. Changing variables

$$x \to z = x + \mathrm{i}\sqrt{|\alpha|} \tag{31}$$

we obtain

$$I_3(\alpha) = I_{3sc}(\alpha)\int_{-\infty}^{\infty} \mathrm{d}z\, p(z) \exp\left(-\mathrm{i}\frac{z^3}{3}\right) \simeq I_{3sc}(\alpha)\frac{1}{N_{MC}}\sum_{k=1}^{N_{MC}} \exp\left(-\mathrm{i}\frac{z_k^3}{3}\right), \tag{32}$$

Table 2
Results of the evaluation of the integral defined in Eq. (26). The symbols have the same meaning as in Table 1

α	S	MC	E	ΔS	ΔMC
10	0.5605	0.5507	0.5584	0.0021	0.008
	0.5605	0.5617	0.5570	0.0035	0.005
5	0.7927	0.8002	0.8104	0.0177	0.01
	0.7927	0.8742	0.8661	0.0734	0.005
1	1.7725	2.0453	2.0201	0.2476	0.03
	1.7725	0.7843	0.7994	0.9731	0.02
0.5	2.5066	2.1587	2.2086	0.2980	0.04
	2.5066	0.6126	0.6146	1.8920	0.04
0.1	5.6050	2.2783	2.3378	3.2672	0.1
	5.6050	0.4228	0.4269	5.1781	0.09

Table 3
Results of the evaluation of the integral defined in Eq. (27). The symbols have the same meaning as in Table 1, but now all values are real

α	S	MC	E	ΔS	ΔMC
10	0.03921	0.04011	0.04024	0.00103	0.00007
5	0.3497	0.3507	0.3508	0.0011	0.00007
1	0.5475	0.5362	0.5356	0.0119	0.001
0.5	0.5051	0.4769	0.4757	0.0294	0.002
0.1	0.4627	0.3772	0.3808	0.0819	0.003

where the distribution function for the Monte Carlo points z_k is

$$p(z) = \frac{|\alpha|^{1/4}}{\sqrt{\pi}} \exp\left(-\sqrt{|\alpha|}\, z^2\right) \tag{33}$$

and

$$I_{3sc}(\alpha) = \frac{1}{2\pi} \exp\left(-\tfrac{2}{3}|\alpha|^{3/2}\right) \int_{-\infty}^{\infty} dz \exp\left(-\sqrt{|\alpha|}\, z^2\right) = \frac{1}{2\sqrt{\pi}|\alpha|^{1/4}} \exp\left(-\tfrac{2}{3}\alpha|^{3/2}\right) \tag{34}$$

is the semiclassical expression.

The results for the calculations can be found in Tables 1–4, where we show, for the real and the imaginary parts, the semiclassical results S, the results using the method described in this Letter, MC, and the exact values E, as well as the semiclassical deviation $\Delta S = |S - E|$ and the statistical error ΔMC obtained by the Monte Carlo calculation. Naturally, the Monte Carlo result will depend slightly on the seed of the random number generator. The same seed was used in all cases. We have also checked, in all cases, that the Monte Carlo results converge to the exact values as $1/\sqrt{N_{MC}}$ as N_{MC} increases.

The numerical tests that we chose include a simple illustration of the method with $I_1(\alpha)$ (only one real stationary point and a rotation of $\pi/4$), a case where a rotation angle significantly smaller than $\pi/4$ is required, a case with two contributing real stationary points and a case with two complex stationary points where one of them does not contribute to the integral. We find that discarding the complex stationary points whenever real stationary points are available seems entirely justified. We also find that the method does not break down if a rotation angle different from $\pi/4$ is used, although Monte Carlo convergence is somewhat slower. This may be necessary for potentials that grow faster than x^4 at infinity.

The results in Tables 1–4 seem to indicate that this method efficiently samples the regions which provide the main contribution to the integrals. The quantum correction with a modest 5000 points Monte Carlo calculation generally decreases the semiclassical error. As expected, the statistical error increases as the parameter α decreases and the semiclassical approximation becomes poorer, although the correction still improves significantly the semiclassical result. Caution should be exerted, however, whenever this method is used to describe a system far from the semiclassical regime.

Table 4
Results of the evaluation of the integral defined in Eq. (27) for negative values of α. The symbols have the same meaning as in Table 1, but now all values are real

α	S	MC	E	ΔS	ΔMC
−10	1.1083×10^{-10}	1.1052×10^{-10}	1.1048×10^{-10}	0.0035×10^{-10}	0.0003×10^{-10}
−5	1.0930×10^{-4}	1.0845×10^{-4}	1.0834×10^{-4}	0.0096×10^{-4}	0.0006×10^{-4}
−1	0.1448	0.1359	0.1353	0.0095	0.0004
−0.5	0.2650	0.2317	0.2317	0.0333	0.001
−0.1	0.4912	0.3293	0.3292	0.1620	0.004

4. Discussion

The method developed in this Letter allows for the Monte Carlo calculation of a real time path integral, by sampling the paths around the classical trajectories with a gaussian distribution function. The final expression (Eq. (22)) gives the quantum path integral as the product of the semiclassical result with an integral which can be evaluated by the Monte Carlo method. Monte Carlo convergence is expected to be good if the semiclassical approach is reasonable, as the function that is being sampled varies smoothly around the stationary path.

It is instructive, at this point, to note that the SPMC, being a very flexible method, can provide a filter function which resembles the gaussian distribution function that we obtained (expression (13)). If we take the probability distribution $P(y)$ in the filter function $D(x)$ to be a gaussian and expand the exponent of the integrand in Eq. (6) of Ref. [5] around the stationary point, keeping only the quadratic terms, then, a choice of

$$\epsilon^2 = \frac{1 - i}{2S_2(x_s)} \tag{35}$$

would produce the appropriate form for $D(x)$. There are two basic differences between our method and this formulation of the SPMC method: the rotation and the absence of the second order term in our sampled function. Due to the rotation, we evaluate the sampled function at the complex points $x_s + z\exp(i\pi/4)$ while in the SPMC method the sampled function is evaluated at the real points $x_s + z$. The second order term in the exponent is, in our method, absent from the sampled function, as it was used to obtain the distribution function. Therefore, only the non-semiclassical terms have to be sampled, thus exhibiting a non oscillatory behaviour near the semiclassical regime. In the SPMC method, the whole function $S(x)$ has to be sampled and the presence of the second order terms will slow down the Monte Carlo convergence.

Our method is more restrictive than the SPMC and other methods that also use the idea of sampling around the classical trajectories [4–8] in so far as it requires that the stationary paths be previously known and well apart from each other. Still, it presents several performance advantages. It does not require the use of a Markov chain, as the gaussian probability distribution can be generated by the Box-Muller method. In this way, it avoids the evaluation of the correlation times [21] and of the normalization. In the multi-dimensional case, our method only requires the diagonalization of a matrix per stationary path. After this diagonalization is performed, the matrix $\mathbf{O}$ is built once and for all and used for all Monte Carlo points in Eq. (22). Finally, the function that is being sampled is non oscillatory in the neighbourhood of the stationary point (it is of fourth order), where the Monte Carlo points lie. Therefore Monte Carlo convergence is expected to be good.

In a scattering problem, the classical trajectories are often few and well apart from each other [18]. In view of its expected good performance, especially for "near semiclassical" systems, and of its light computational demands, this method should provide an appropriate tool to obtain quantum corrections to the semiclassical results for scattering processes. Work in this direction is now in progress.

References

[1] D.M. Brink, Semi-Classical Methods for Nucleus-Nucleus Scattering (Cambridge University Press, Cambridge, 1985).
[2] D. Thirumalai, B.J. Berne, Chem. Phys. Letters 116 (1985) 471.
[3] V.S. Filinov, Nucl. Phys. B 271 (1986) 717.
[4] N. Makri, W.H. Miller, Chem. Phys. Letters 139 (1987) 10.
[5] J.D. Doll, D.L. Freeman, M.J. Gillan, Chem. Phys. Letters 143 (1988) 277.
[6] J.D. Doll, T.L. Beck, D.L. Freeman, J. Chem. Phys. 89 (1988) 5753.
[7] N. Makri, W.H. Miller, J. Chem. Phys. 89 (1988) 2170.
[8] N. Makri, Comp. Phys. Comm. 63 (1991) 389.
[9] C.H. Mak, D. Chandler, Phys. Rev. A 41 (1990) 5709.
[10] C.H. Mak, D. Chandler, Phys. Rev. A 44 (1991) 2352.

[11] J. Chang, W.H. Miller, J. Chem. Phys. 87 (1987) 1648.
[12] J.D. Doll, R.D. Coalson, D.L. Freeman, J. Chem. Phys. 87 (1987) 1641.
[13] N. Makri, Chem. Phys. Letters 159 (1989) 489.
[14] C.H. Mak, Phys. Rev. Letters 68 (1992) 899.
[15] D.J. Kouri, W. Zhu, X. Ma, B.M. Pettitt, D.K. Hoffman, J. Phys. Chem. 96 (1992) 9622.
[16] D.J. Kouri, Y. Huang, D.K. Hoffman, Phys. Rev. Lett. 75 (1995) 49.
[17] A.C. Gentile, D.A. Evensky, J.L. Durant, J. Chem. Phys. 105 (1996) 7613.
[18] F.D. dos Aidos, D.M. Brink, J. Phys. G: Nucl. Phys. 11 (1985) 249.
[19] R.P. Feynman, A.R. Hibbs, Quantum Mechanics and Path Integrals (McGraw-Hill, New York, 1965).
[20] L.S. Schulman, Techniques and Applications of Path Integration (Wiley, New York, 1981).
[21] A.D. Sokal, Monte Carlo Methods in Statistical Mechanics: Foundations and New Algorithms, Cours de Troisième Cycle de la Physique en Suisse Romande (Lausanne, June 1989).